ANALYTICAL STUDY OF A LAMINAR DIFFUSION FLAME RESPONSE TO SIMULTANEOUS FLUCTUATIONS OF INLET MASS FRACTION AND FLOW VELOCITY

Ali Khosousi*, Farhad Fathieh*, Mohammad Farshchi*, Akbar Ghafourian*
E-mail: a_khosousi@ae.sharif.edu
*Aerospace Department, Sharif University of Technology, Tehran, Iran

Abstract
The unsteady response of a laminar diffusion flame to harmonic mass fraction oscillations and also flow velocity fluctuations has been investigated. Flame-sheet assumption is utilized to model the laminar unsteady two-dimensional co-flow diffusion flame mathematically. The initial combustion of most combustion chambers is through diffusion mechanism. Therefore, developing analytical model of diffusion combustion is of great importance. The flow is assumed subsonic (incompressible), inviscid, and uniform. The convection-diffusion equation for conserved scalar variable with appropriate boundary conditions is solved. Considering stoichiometric mass fraction surface to be the flame surface, it is possible to obtain the flame zone. In addition, different types of flame structures and transition from overventilated flame to underventilated flame are studied. Assuming that unburnt species have not passed across the flame surface and that the diffusion coefficient is constant, heat release rate can be considered proportionate to flame area. This method, for the first time in this work, is applied to diffusion flames to calculate heat release rate. Heat release rate oscillations, in the form of flame response function to fuel mass fraction fluctuations, flow velocity perturbations, and the simultaneous fluctuations of mass fraction and flow velocity, for the first and the second modes are acquired. At each Peclet number, frequency domain is divided into three regions, diffusion-dominant region, convection-diffusion region, and convection-dominant region. The obtained results indicate that the magnitude of response function decreases as excitation frequency increases, while phase difference approaches a constant value.

Keywords: *Diffusion flame, Mass fraction oscillations, Heat release rate, Flame structure, Response function*

Introduction
Almost all the devices producing power utilize combustion process which takes place in burners. Because of safety issues in storing and transporting combustible mixture, diffusion flame is more applicable even though it produces much more pollutant per unit of heat release rather than premixed flame. Thus, many works have been conducted to investigate the physics of diffusion flame.

The earliest analytical solution to the laminar jet flame problem was conducted by Burke and Schumann [1]. In this work co-flow fuel and oxidizer streams enter a cylindrical duct. This problem is solved for both axisymmetric and two-dimensional configurations, the flame-sheet approximation is used and the stoichiometric surface is considered as the flame surface.

In as much as excellent accordance of Burke-Schumann model with experimental observations, many works carried out in order to extend this model [2-6]. Furthermore, many experimental works have been done to study co-flow diffusion flames [7-9].

Fay [2] solved the laminar jet flame problem with variable-density assuming unit Schmidt and Lewis numbers and absolute viscosity, directly proportional to temperature. Combustion process can be affected adversely by instabilities. These instabilities come from interactions

between oscillatory flow and heat release process which lead to enhanced vibrations, reduced part life, flame blow-off or flash-back, and even complete failure of system. As a result, a large number of surveys have been carried out to find out more about combustion instabilities and its origin, especially in premixed flames which responds more intensely to perturbations comparing to diffusion flames [12].

Tyagi et al. [11] numerically studied an unsteady non-premixed flame in a uniform flow field, based on the Burke–Schumann geometry with examination of both finite and infinite chemical reaction rate. Timothy et. al. [12] experimentally investigated the response of diluted 2-D methane-air and ethylene-air diffusion flames to acoustic pressure fluctuations in a wide range of frequencies and for low and medium pressure regimes.

Using analytical and numerical techniques, Tyagi et al. [13] have recently studied the unsteady response of a nonpremixed flame in the same framework as Burke–Schumann problem. The heat release response of a two-dimensional (2-D) co-flow diffusion flame was studied. The results show that the flame response strongly depends on excitation frequency so that the flame responds only to low frequency perturbations, almost below 10 Hz. This frequency is far lower in comparison to the frequencies at which premixed flames respond, however, both flames behave in a similar manner.

The present work is an extension to Tyagi et. al. [13] studies and presents an analytical solution for the cases of flow velocity perturbations and the combination of velocity and mixture fraction fluctuations; whereas in the previous work [13] the whole solution was obtained numerically. In addition to exact solutions, the method of acquiring heat release rate is the main difference between present work and previous works. This model has not been applied to diffusion flames before. Although the method applied to this problem to compute heat release rate is completely distinct from Tyagi [13], the results have a remarkable correspondence and the trend of response function obtained for heat release rate as a response to mass fraction and velocity perturbations is similar.

Formulation

In this work, the 2-D unsteady diffusion flame has been modeled. The geometry is schematically displayed in Fig. 1. In this configuration, fuel is supplied through the inner slot and oxidizer through the outer slot. The flow is laminar, subsonic (incompressible), the effects of viscosity are neglected, and boundaries are rigid. The velocity field is axial and spatially uniform and also diffusion coefficient is constant. In addition, flame is a symmetric surface attached to the rim of the fuel slot. The mixing field can be expressed by the convection-diffusion equation for Schwab–Zel'dovich variable, in two-dimensional Cartesian coordinate system as follow:

$$\frac{\partial Z}{\partial \hat{t}} + \hat{u}\frac{\partial Z}{\partial \hat{x}} = D\left(\frac{\partial^2 Z}{\partial \hat{x}^2} + \frac{\partial^2 Z}{\partial \hat{y}^2}\right), \tag{1}$$

where Schwab–Zel'dovich variable is defined as $Z = \alpha_F - \alpha_A$. In addition $\alpha_F = -Y_F/W_F\nu'_F$ and $\alpha_A = -Y_A/W_A\nu'_A$ are normalized mass fractions of fuel and oxidizer respectively. "^" indicates dimensional parameters. Using L and U respectively as characteristic length and velocity, the non-dimensionalized equation is:

$$\frac{\partial Z}{\partial t} + u\frac{\partial Z}{\partial x} = \frac{1}{Pe}\left(\frac{\partial^2 Z}{\partial x^2} + \frac{\partial^2 Z}{\partial y^2}\right), \tag{2}$$

where $Pe = UL/D$ is the dimensionless Peclet number. Boundary conditions applied to this equation are as follows:

$$Z=\begin{cases}-\alpha_{A_i} & x=0,\quad \delta<y<1\\ \alpha_{F_i} & x=0,\quad 0<y<\delta\end{cases}, \tag{3.a}$$

$$\frac{\partial Z}{\partial y}=0 \quad y=1, \tag{3.b}$$

$$\frac{\partial Z}{\partial y}=0 \quad y=0, \tag{3.c}$$

$$\frac{\partial Z}{\partial x}=0 \quad x\to+\infty\cdot \tag{3.d}$$

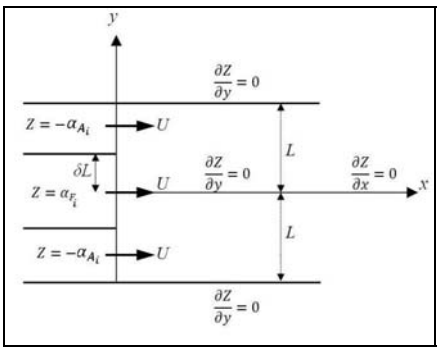

Figure 1. Schematic of the combustion zone

Eq. (3.a) is expressive of inlet mass fraction in which α_{A_i} and α_{F_i} are inlet mass fractions of oxidizer and fuel respectively. Eq. (3.b) satisfies impenetrability of the upper and lower boundaries and Eq. (3.c) is resulted from the symmetry of the flame. And Eq. (3.d) is because of the absence of perturbations at infinity. By identifying the velocity field and appropriate boundary conditions, Eq. (2) has an exact solution. Velocity field and mass fraction are regarded as the summation of a steady and a time-dependent term $u=\overline{u}+u'$ and $\alpha=\overline{\alpha}+\alpha'$.

Since Eq. (2) is linear, Schwab–Zel'dovich variable, *Z(x,y,t)*, can also be taken down as summation of a steady and a time-dependent term $Z=\overline{Z}+Z'$. Consequently, by neglecting higher order non-linear terms, two equations for steady and unsteady states are resulted:

$$\frac{\partial\overline{Z}}{\partial t}+\overline{u}\frac{\partial\overline{Z}}{\partial x}=\frac{1}{Pe}\left(\frac{\partial^2\overline{Z}}{\partial x^2}+\frac{\partial^2\overline{Z}}{\partial y^2}\right), \tag{4}$$

$$\frac{\partial Z'}{\partial t}+\overline{u}\frac{\partial Z'}{\partial x}+u'\frac{\partial\overline{Z}}{\partial x}=\frac{1}{Pe}\left(\frac{\partial^2 Z'}{\partial x^2}+\frac{\partial^2 Z'}{\partial y^2}\right)\cdot \tag{5}$$

Inlet fuel and oxidizer mass fraction fluctuations and also velocity perturbations are considered harmonic with excitation angular frequency ω and specified amplitude $u'=\widetilde{u}e^{i(\omega t+\phi)}$, $\alpha_{A_i}=\overline{\alpha}_{A_i}+\widetilde{\alpha}_{A_i}e^{i\omega t}$, and $\alpha_{F_i}=\overline{\alpha}_{F_i}+\widetilde{\alpha}_{F_i}e^{i\omega t}$. Assuming constant steady velocity field, $\overline{u}=1$, and harmonic Z' fluctuations with excitation frequency, $Z'=\widetilde{Z}e^{i\omega t}$, following equation is obtained:

$$\frac{\partial^2\widetilde{Z}}{\partial x^2}+\frac{\partial^2\widetilde{Z}}{\partial y^2}-Pe\frac{\partial\widetilde{Z}}{\partial x}-Pei\omega\widetilde{Z}=Pe\widetilde{u}e^{i\phi}\frac{\partial\overline{Z}}{\partial x}\cdot \tag{6}$$

By exerting boundary conditions, subsequent results are acquired:

$$Z=\overline{Z}+Z', \tag{7}$$

$$\overline{Z}=\delta(\overline{\alpha}_{F_i}+\overline{\alpha}_{A_i})-\overline{\alpha}_{A_i}+2(\overline{\alpha}_{F_i}+\overline{\alpha}_{A_i})\sum_{n=1}^{\infty}\frac{\sin(n\pi\delta)}{n\pi}\exp(S_{1,n}x)con(n\pi y), \tag{8}$$

$$Z'(x,y,t)=\left\{\sum_{n=0}^{\infty}\left(A_n\exp(S_{2,n}x)+M_n\exp(S_{1,n}x)\right)con(n\pi y)\right\}e^{i2\pi ft}, \tag{9}$$

in which:

$$S_{1,n} = \frac{1}{2}\left(Pe - \sqrt{Pe^2 + 4n^2\pi^2}\right), \tag{10}$$

$$S_{2,n} = \frac{1}{2}\left(Pe - \sqrt{Pe^2 + 4n^2\pi^2 + 8iPe\pi f}\right), \tag{11}$$

$$A_0 = \delta\left(\tilde{\alpha}_{F_i} + \tilde{\alpha}_{A_i}\right) - \tilde{\alpha}_{A_i}, \tag{12}$$

$$A_n = 2\left(\tilde{\alpha}_{F_i} + \tilde{\alpha}_{A_i}\right)\frac{\sin(n\pi\delta)}{n\pi} - M_n. \tag{13}$$

Since, in order to solve Eq. (6) complex notation has been put to work; only the real part of Z must be taken into account. Considering mixed-is-burnt and flame sheet in Burke-Schumann model, it is possible to consider stoichiometric surface which is the very locus of $Z = 0$, the flame surface. Therefore, the identification of the simultaneous flame shape at any frequency is possible. In the vicinity of the flame surface, where the temperature is extremely high, chemical kinetics takes place rapidly [14]. Taking the advantage of fast chemical kinetics assumption, the very flame surface is where the heat release occurs. By assuming that the unburnt species do not pass across the flame surface, the heat release rate can be expressed as $dq = \rho V_D \Delta h_r dA_f$, where V_D is diffusion velocity, Δh_r is heat of reaction per unit mass of mixture, and A_f is the area of flame surface. Making use of constant diffusion velocity and flow density, and also specifying the fuel type (Specified Δh_r) heat release rate will be proportional to the area of flame surface $dq \propto A_f$. By finding the instantaneous area of flame surface at each frequency, heat release rate is obtainable. Since the relationship between heat release rate oscillations and entrance perturbations is nonlinear, higher modes appear here and a response function for each harmonic has to be defined. Entrance perturbations are in the form of $\tilde{C}e^{i\omega t}$, where $\tilde{C}$ is perturbation amplitude and ω is excitation angular frequency. If it is assumed that the flame responds at the same excitation frequency [15], due to the presence of higher harmonic modes, instantaneous heat release rate can be written as a Fourier series expansion in time $q = \bar{q} + \sum_{n=1}^{\infty} \tilde{q}_n e^{i(n\omega t + \phi_n)}$ in which $\tilde{q}_n$ and φ_n are magnitude and phase difference of response function for nth harmonic respectively.

Before presenting the results, it is necessary to express Peclet number as the ratio of diffusion time scale ($\hat{\tau}_D = L^2/D$) to convection time scale ($\hat{\tau}_C = L/U$). By defining convection frequency as $\hat{f}_C = 1/\hat{\tau}_C$ and also diffusion frequency as $\hat{f}_D = 1/\hat{\tau}_D$, it is possible to say that Peclet number is the ratio of these two frequencies $Pe = \hat{\tau}_D/\hat{\tau}_C = \hat{f}_C/\hat{f}_D$.

Using L and U, diffusion and convection frequencies can be non-dimensionalized as $f_C = 1$ and $f_D = 1/Pe$. According to above-mentioned definitions, flame oscillations with respect to non-dimensionalized excitation frequency can be classified into three categories:

1. $f > f_C$, convection-dominant region, in which oscillation time scale is lower than convection time scale.
2. $f_D < f < f_C$, convection-diffusion region, in which oscillation time scale is between diffusion time scale and convection time scale.
3. $f < f_D$, diffusion region, in which oscillation time scale is higher than diffusion time scale.

Response to mass fraction fluctuations

The present section studies the diffusion flame response to fuel mass fraction fluctuations. Fuel slot width has been selected in a way which brings about the formation of a steady overventilated flame [14] and therefore $\delta = 0.1$. Steady values of fuel and oxidizer mass

fractions at the inlet, similar to Tyagi et al. [13], are chosen as $\overline{\alpha}_{F_i} = 3.2$ and $\overline{\alpha}_{A_i} = 3.2/7$, respectively. Based on experimental methods to measure air (oxidizer) flow rate, for example using sonic nozzle, oxidizer mass fraction is practically constant and so $\widetilde{\alpha}_{A_i}/\overline{\alpha}_{A_i} = 0$. The ratio of fuel mass fraction to its steady value is $\alpha_r = \widetilde{\alpha}_{F_i}/\overline{\alpha}_{F_i} = 0.1$, *0.2*, *0.3*, and *0.5*.

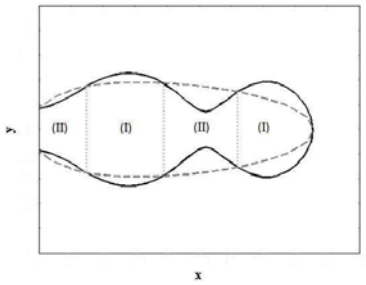

Figure 2. High (I) and low (II) concentration regions in the flame

Along with harmonic oscillations of fuel mass fraction, a high concentration region, in which fuel mass fraction is high, and a low concentration region, in which fuel mass fraction is low, are formed which result in flame wrinkles. These two regions propagate as a wave with the flow velocity. Fig. 2 schematically depicts these high (I) and low (II) concentration regions. Because of the transverse diffusion and propagation of the wave, in high concentration regions, fuel transverse movement causes augmentation in the amplitude of the flame wrinkles. After moving forward and decreasing in fuel concentration, oxidizer begins to diffuse into fuel and this highly concentrated region slowly burns away. On the other hand, in low concentration regions into which the surrounding oxidizer diffuses, the amplitude of the wrinkles is steadily decreasing. Disappearance of the low concentration region between two high concentration regions leads to flame clip-off. During this phenomenon, the high concentration region like a fuel mass advances in the flow field up to the point where the entire fuel is burnt. Fig. 3 shows the stoichiometric flame surface together with the flame clip-off during a cycle for $f = 0.5$, $\alpha_r = 0.5$, and $Pe = 10$. As the amplitude of the perturbations and subsequently flame wrinkles increases, the flame clip-off formation is more probable. Not only perturbations, but also diffusion time scale brings about flame clip-off. Diffusion time scale has inverse relationship with excitation frequency. The lower the excitation frequency, the more time the oxidizer will have to diffuse into low concentration region travelling with the flow velocity. Therefore, at any constant Peclet number, flame clips off only below a certain excitation frequency. This frequency must be lower than characteristic flow frequency.

In Fig. 4, with the decrease of the frequency to $f = 0.1$, the flame is underventilated over some short time spans of the cycle. In this situation, fuel, to diffuse into oxidizer, has adequate amount of time to touch the walls. With the disappearance of low concentration region, clip-off occurs in part of the flame and the remaining flame will be underventilated for a short period. The underventilated part clips off again and a small part of the flame, which is left overventilated, grows again and eventually returns to the beginning of the cycle.

The study of unsteady flames is applicable to the combustion instabilities and for this reason the identification of the flame response to unsteady excitation is of paramount importance. Flame response is defined as the ratio of the magnitude of heat release rate ($\widetilde{q}_n$) oscillations to mass fraction changes. In this section, flame response is analytically investigated as a response function of heat release rate to fuel mass fraction fluctuations at the fuel-slot inlet. For this reason, the response of heat release rate is achieved for various ratios of amplitude of inlet fuel mass fraction fluctuations to its steady value, $\alpha_r = 0.1$, *0.2* and *0.3*.

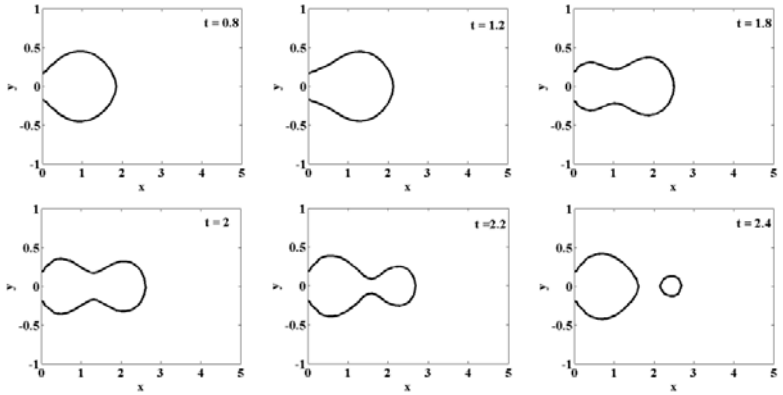

Figure 3. Flame shape at different time in a cycle at $f = 0.5$, $\alpha_r = 0.5$, and $Pe = 10$

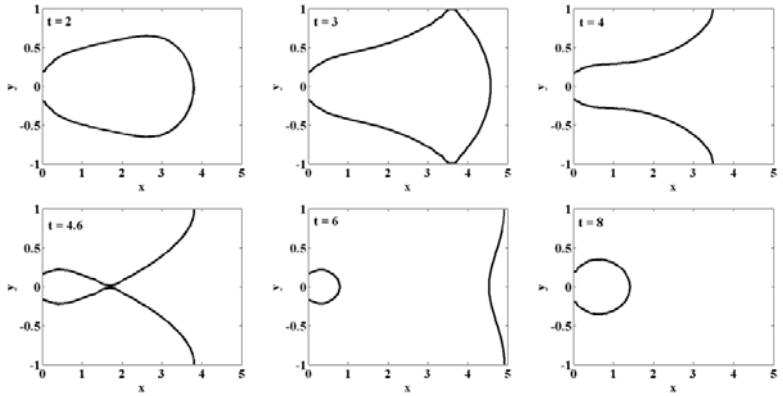

Figure 4. Flame shape at different time in a cycle at $f = 0.1$, $\alpha_r = 0.5$, and $Pe = 10$

Fig. 5.a and Fig. 5.b respectively show the magnitude and the phase of the first harmonic of response function with respect to excitation frequency. It can be observed that the magnitude of the first mode, by going closer to the convection frequency ($f_C = 1$), independent from amplitude of perturbations, is constantly decreasing to the point where $f > 1$, it almost approaches zero. This magnitude decrease behavior, with the increase of excitation frequency, is in accordance with the results of diffusion flames [13] as well as premixed flames [10]. When $f < f_D$, because of the domination of diffusion on convection, the flame responds significantly to fuel mass fraction fluctuations. As perturbation amplitude (α_r) increases, the magnitude of first mode increases at low frequencies. Fig. 5.b shows that the first harmonic phase is constantly negative which is an indication of the time lag of heat release rate oscillations behind the fuel mass fraction fluctuations. For frequencies lower than diffusion frequency, $f < 0.1$, phase difference, independent from the amplitude of fuel mass fraction fluctuations, increases dramatically. Besides, in near zero frequencies, the phase difference is insignificant which expresses quasi-steady behavior and prompt response of the flame. On the other hand, it can be observed that in convection-dominant region, $f > 1$, phase difference for various amplitudes approaches a constant value of about 270^o. In convection-diffusion region, $0.1 < f < 1$, a dramatic increase at intermediate frequencies forms a peak. Fig. 5.c depicts the magnitude of the second mode which is approximately one order smaller than that of the first mode. Similar to the first mode, with the increase in excitation frequency, the magnitude approaches zero. Furthermore, with the increase of the amplitude of fluctuations, the magnitude of the response increases as well. It is observed that at about $f = 0.1$, which is equal to diffusion timescale, the magnitude increases locally and again forms a peak. The reason for such phenomenon can be attributed to the coupling between axial diffusion and excitation fre-

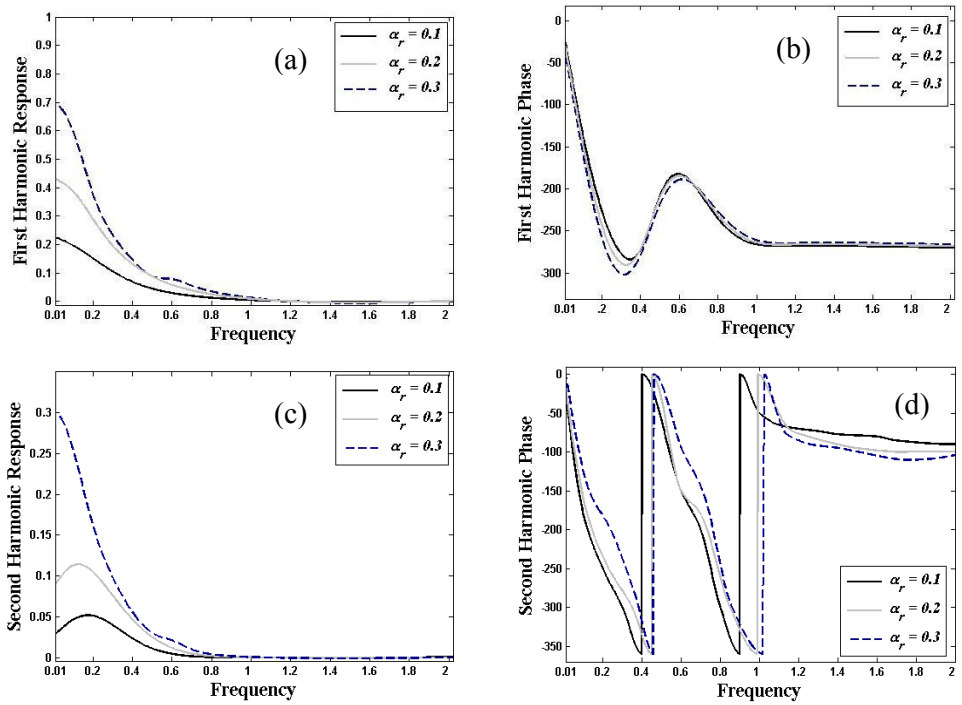

Figure 5. Response function of heat release rate with respect to fuel mass fraction fluctuations as a function of excitation frequency for different amplitudes of excitation

quency, which results in an abrupt change in the flame length. As the amplitude of the excitations increases, aforementioned peak moves toward the lower frequencies.

The second harmonic phase is also similar to the first phase, as shown in Fig. 5.d. The second phase is unimportant at near zero frequencies which is resulted by the quasi-steady behavior of the flame. At the higher than 1 frequencies, the phase approaches toward a constant value of about 90^o. It can be seen that heat release rate becomes in phase with fuel mass fraction fluctuations twice in convection-diffusion region. As amplitude of fluctuations increases, the frequency at which heat release rate is in phase with fuel mass fraction fluctuations goes up slightly.

Response to velocity fluctuations

In this section the influence of time independent spatially uniform velocity fluctuations will be discussed. Similar to previous section, the values, of the various parameters are chosen as $\overline{\alpha}_{F_i} = 3.2$, $\overline{\alpha}_{A_i} = 3.2/7$ and $\delta = 0.1$. The ratio of the amplitude of the velocity fluctuations to its steady state value is selected as $U_r = \tilde{u}/\overline{u} = 0.1$, 0.3, and 0.5.

The ratio of convection to diffusion timescales, with harmonic oscillations of the velocity field, goes up and down with time. In fact, when the instantaneous flow velocity rises, the residence time shortens and fuel, in order to diffuse into oxidizer, needs more axial distance. Consequently, the flame length increases. Likewise, the flame length decreases as the instantaneous flow velocity decreases. Fig. 6 displays the effects of velocity fluctuations on the flame shape at $f = 0.5$ and $U_r = 0.5$. In this case, the flame length varies between 2.1 and 2.4. Fig. 6 shows the flame shape at the lower frequencies corresponding to diffusion timescale $f = 0.1$. The flame length varies between 1.5 to 3, which perfectly shows more intense flame response at lower frequencies.

It was observed that the main effect of fuel mass fraction fluctuations was the appearance of wrinkles on the flame surface resulting from transverse diffusion. Such phenomenon,

however, is not seen in the presence of the velocity fluctuations whose dominant effects are only on the flame length. Furthermore in this case, flame clip-off and flame structure transition from being overventilated to being underventilated are not observed.

Fig. 7 shows response function of heat release rate for various amplitudes of velocity fluctuations for *Pe = 10*. In Fig. 7.a, the magnitude of the first harmonic mode for all amplitudes of fluctuations decreases with a rise in frequency. In diffusion as well as intermediate convection-diffusion regions, this decrease occurs at a higher rate to the point where it reaches a minimum value at $f = 0.7$. In addition, in convection-dominant region, similar to fuel mass fraction fluctuations, the magnitude of the first mode becomes zero.

With the increase of the amplitude of the velocity fluctuations, the magnitude of first harmonic mode rises distinctly. Fig. 7.b displays the first harmonic phase. As it can be observed that at all frequencies, the phase is negative which expresses the time lag of heat release rate behind velocity fluctuations. At very low frequencies, the phase difference is about zero and therefore the flame responds immediately to perturbations. In diffusion-dominant region, $f < f_D$, the increase of the amplitude of the velocity fluctuations has no effect on phase difference and with the increase of the frequency, phase difference increases. In convection-diffusion region, $f_C < f < f_D$, the increase of the amplitude of the perturbations leads to a small forward shift in phase difference and eventually in convection-dominant region, the phase difference for all velocity fluctuation amplitudes approaches a constant value.

Fig. 7.c shows the magnitude of the second harmonic mode. Since the magnitude of the second mode, in comparison to that of the first mode, is very small, it is possible to fit the heat release rate oscillations with a sine function. In diffusion- dominant region, a maximum, due to axial diffusion, is seen. There is also, in convection- diffusion region, a small maximum at

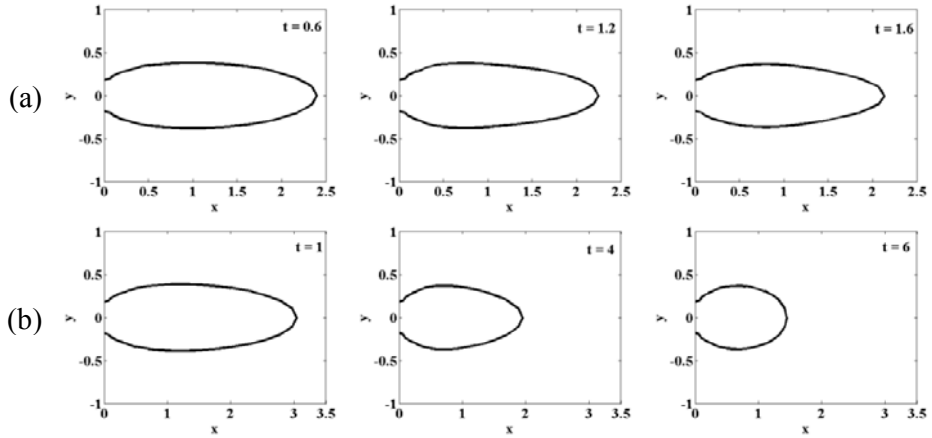

Figure 6. Flame shape at different time in a half cycle for $U_r = 0.5$ at a) $f = 0.5$ b) $f = 0.1$

$f = 0.7$, which precisely corresponds to the minimum observed in the magnitude of the first mode. The influence of the increase in the amplitude of the velocity fluctuations on the magnitude of the second mode is similar to that of the first mode. Fig. 7.d shows the second harmonic phase difference. The slope is generally larger than the first phase and results in more cycles. At higher frequencies second phase difference approaches a constant value.

Response to simultaneous fluctuations of inlet mass fraction and flow velocity

In this section the simultaneous effects of fuel mass fraction and velocity fluctuations are to be examined. In addition, the phase difference between these two parameters (φ) is considered. Parameters $\overline{\alpha}_{F_i} = 3.2$, $\overline{\alpha}_{A_i} = 3.2/7$ and $\delta = 0.1$ have the same values as the previous

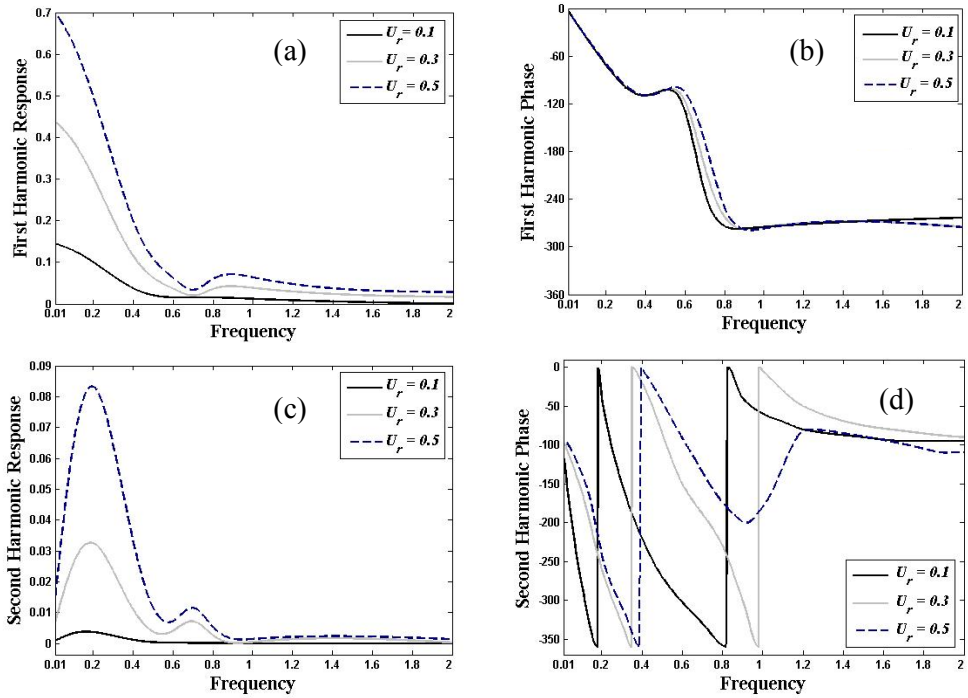

Figure 7. Response function of heat release rate with respect to velocity fluctuations as a function of excitation frequency for different amplitudes of excitation

sections. In this case, the ratio of the amplitude of fuel mass fraction fluctuations to its steady value equals $\alpha_r = 0.3$ and the ratio of the amplitude of the velocity fluctuations to its steady value equals $U_r = 0.5$. The effect of φ is studied for three different values 0^o, 90^o, and 180^o.

In the two previous sections, it was observed that the major consequence of the fuel mass fraction excitations is wrinkle formation, clip off, and flame transition from being overventilated to being underventilated. Also, flow velocity fluctuations have conspicuous effect on the flame length. Therefore, with concurrent excitation of these two parameters all of such phenomena are observed.

The Stoichiometric flame surface is obtained in a cycle at $f = 0.5$ with $U_r = 0.5$, $\alpha_r = 0.5$, $Pe = 10$, and $\varphi = 90^o$, Fig. 8. The wrinkles observed on the flame surface are due to fuel mass fraction fluctuations which indicate the flame structure is more sensitive to mass fraction fluctuations than velocity perturbation. By increasing phase difference to $\varphi = 180^o$, the time when clip off starts decreases and the size of detached part increases, Fig. 9. As a consequence, the phase difference between fuel mass fraction and velocity fluctuation on flame structure influences the start time and the size of clip-off.

Fig. 10 shows the response function of heat release rate with respect to simultaneous fuel mass fraction and flow velocity fluctuations as a function of excitation frequency. Fig. 10.a shows the magnitude of the first harmonic mode versus frequency for three values of $\varphi = 0^o$, 90^o, and 180^o is depicted. The magnitude of the first harmonic mode for $\varphi = 0^o$ and 90^o decreases as frequency increases while a different behavior can be seen for $\varphi = 180^o$ as a peak formation at the diffusion-dominant region. In general, as the phase difference between fuel mass fraction and flow velocity increases, the magnitude of the response function goes down.

Fig. 10.b shows the phase of the first harmonic mode. At low frequencies, in diffusion-dominant region, the phase difference for $\varphi = 0^o$ and 180^o is zero; in fact the flame responds to the fluctuations rapidly. While in $\varphi = 90^o$, in diffusion dominant region, phase difference has nonzero value. In convection-dominant region, the phase difference for $\varphi = 0^o$ and 180^o tends

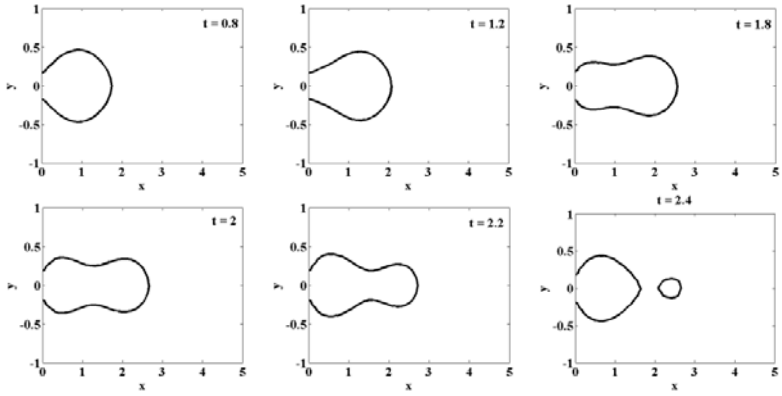

Figure 8. Flame shape at different time in a cycle at $f = 0.5$, $\alpha_r = 0.5$, $U_r = 0.5$, and $\varphi = 90^o$

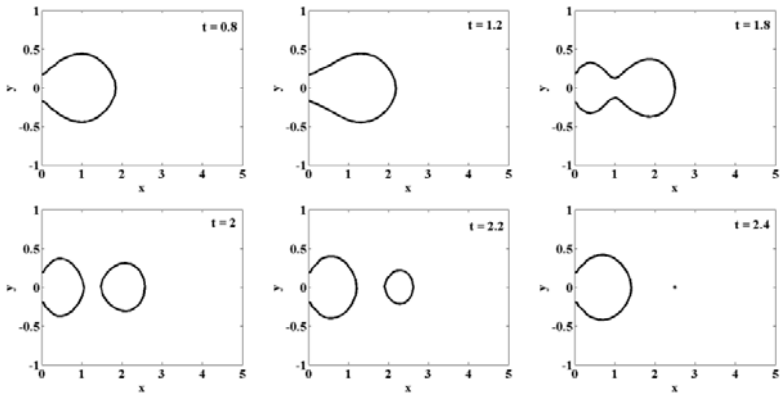

Figure 9. Flame shape at different time in a cycle at $f = 0.5$, $\alpha_r = 0.5$, $U_r = 0.5$, and $\varphi = 180^o$

to approach to the same constant value, whereas for $\varphi = 90^o$ this very value is smaller.

Fig. 10.c shows the magnitude of the second harmonic mode versus frequency. It was discussed in the previous section that the magnitude of the second harmonic mode for the velocity fluctuation is in a low order which is why for $\varphi = 0^o$ the curve is almost similar to Fig. 5.c with $\alpha_r = 0.3$. The magnitude of the second harmonic mode compared to that of the first mode is by far larger. The behavior of the second mode for $\varphi = 90^o$ is similar to its first mode and the magnitude has just gone down slightly. Fig. 10.d shows the second harmonic phase. At low frequencies, the phase difference for three values of φ is zero and it approaches a constant value at higher frequencies.

Conclusion

This paper examines the unsteady response of a laminar diffusion flame to harmonic mass fraction oscillations and also to flow velocity fluctuations in three cases of: I) only mass fraction fluctuations, II) only flow velocity fluctuations, and III) both mass fraction and flow velocity fluctuations together for three phase difference between inlet perturbations. The Burke-Schumann 2-D symmetric configuration has been applied where fuel and air enter mixing chamber through two inner and outer coaxial slots, respectively. It is assumed that the flow is incompressible, uniform, and inviscid. The transverse component of velocity is neglected and only axial velocity is considered. Consequently, diffusion is the only mechanism for mixing where diffusion coefficient is taken constant within the domain. With the presence of small mass fraction and velocity perturbations, mixing equation have been solved and as a result the Schwab–Zel'dovich variable has been found all over the mixing field . Regarding mixed-is-burnt assumption, the flame surface structure obtained as a locus of

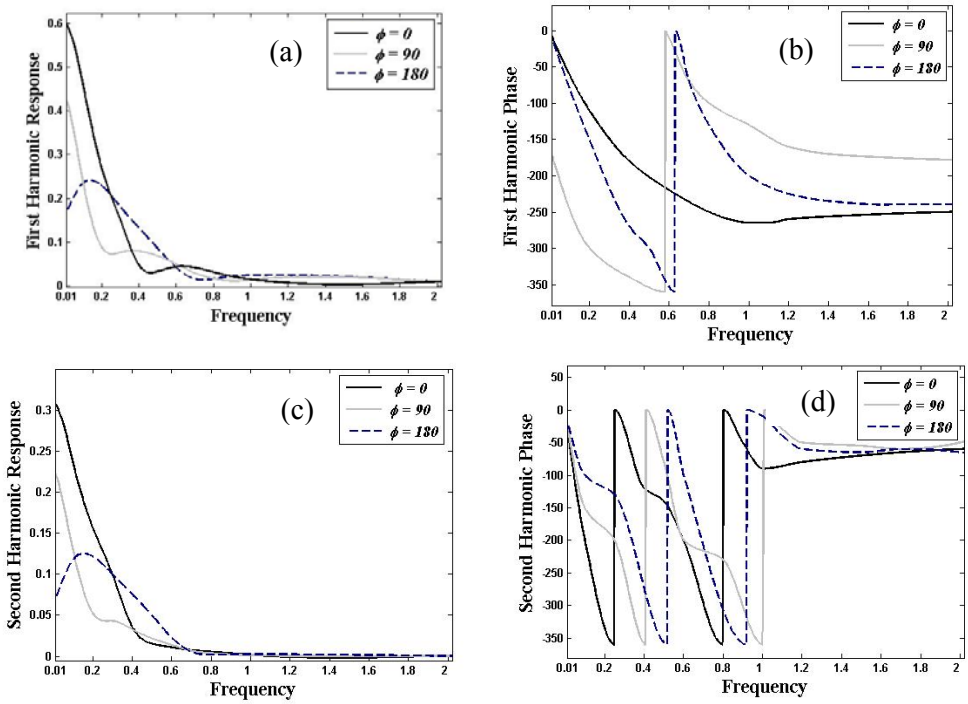

Figure 10. Response function of heat release rate with oscillations of fuel mass fraction and flow velocity as a function of excitation frequency for $\varphi = 0^o, 90^o, 180^o, \alpha_r = 0.3, U_r = 0.5$

stoichiometric points. The results show that the main effect of mass fraction fluctuations on the flame structure is wrinkling. In addition, flame clip-off is seen at higher amplitude of perturbations. As the frequency reduces, the transitions between overventilated and underventilated flame is observed. On the other hand, the flame responds to flow velocity fluctuations in the form of the flame length variations which is more intense in lower frequencies. In this case, flame wrinkling, clip-off, and overventilated to underventilated transition have not been seen. When both mass fraction oscillations and flow velocity fluctuations are present, not only flame wrinkling and clip-off occur but also the flame length varies.

With the assumption that heat release rate is proportional to the flame surface area, which is normally used for premixed flame, the flame heat release rate response to mass fraction oscillations and flow velocity fluctuations with respect to excitation frequency is found. It is seen that flame responds differently in distinct frequency regions, known as convection-dominant region, $f > f_C$, diffusion-dominant region, $f < f_D$, and convection-diffusion region, $f_D < f < f_C$. In all three cases, the increase in amplitude of perturbations causes the magnitude of response to increase which approaches zero as the excitation frequency rises up to convection region. In addition, the phase of flame response is always negative which indicates that heat release lags behind perturbations. In convection-dominant region, the phase reaches a constant value which is different for each amplitude. When the perturbations are only from flow velocity oscillations, it is seen that the magnitude of the second mode is insignificant so that the heat release rate can be fitted by a sinusoidal function. For the third case, by an increase in inlet phase difference between inlet perturbations, the magnitude of response decreases. There are some differences between the present results and Tyagi et. al [13]. In accordance with present work, magnitude of the first mode goes up as amplitude of inlet mass oscillations increases which is physically acceptable; however, it is in contrast with the results obtained by Tyagi [13]. Besides these differences, the whole behaviors of response functions are similar in

both works whereas a shift in values can be seen. This shifting results from difference in heat release modeling. As a matter of fact, a large number of issues about diffusion flames instabilities have yet to be found. Reducing some assumptions applied in this work, such as uniform pattern, would lead to more precise results.

References

[1] Burke, S.P., Schumann, T.E.W., "Diffusion Flames", *Indust. Eng. Chem.*, 20: 998-1004 (1928).

[2] Fay, J.A., "The Distributions of Concentration and Temperature in a Laminar Jet Diffusion Flame", *Journal of Aeronautical Sciences*, 21: 681-689 (1954).

[3] Roper, F.G., "The Prediction of Laminar Jet Diffusion Flame Sizes: Part I. Theoretical Model", *Combustion and Flame*, 29: 219-226 (1977).

[4] Roper, F.G., Smith, C., and Cunningham, A.C., "The Prediction of Laminar Jet Diffusion Flame Sizes: Part II. Experimental Verification", *Comb. and Flame*, 29: 227-234 (1977).

[5] Roper, F.G., "Laminar Diffusion Flame Sizes for Curved Slot Burners Giving Fan-shaped Flames", *Comb. and Flame*, 31: 251-259 (1978).

[6] Khosid, S., Greenburg, J.B., "The Burke–Schumann Spray Diffusion Flame in a Nonuniform Flow Field", *Comb. and Flame*, 118: 13-24 (1999).

[7] Smyth, K.C., Miller, J.H., Dorfman, R.C., Mallard, W.G., and Santoro, R.J., "Soot Inception in a Methane/Air Diffusion Flame as Characterized by Detailed Species Profiles", *Comb. and Flame*, 62: 157-181 (1985).

[8] Oldenhof, E., Tummers, M.J., van Veen, E.H., Roekaerts, D.J.E.M., "Ignition kernel formation and lift-off behaviour of jet-in-hot-coflow flames", *Comb. and Flame*, 157: 1167-1178 (2010).

[9] Joo, H.I., Gülder, Ö.L., "Experimental study of soot and temperature field structure of laminar co-flow ethylene–air diffusion flames with nitrogen dilution at elevated pressures", *Comb. and Flame*, 158: 416-422 (2011).

[10] Fleifel, M., Annaswamy, A.M., Ghoniem, Z.A., and Ghoniem, A.F., "Response of a Laminar Premixed Flame to Flow Oscillations: A Kinematic Model and Thermoacoustic Instability Results", *Comb. and Flame*, 106: 487-510 (1996).

[11] Tyagi, M., Chakravarthy, S.R., and Sujith, R.I., "Unsteady Combustion Response of a Ducted Non-premixed Flame and Acoustic Coupling", *Combust. Theory Mod.*, 11(2): 205-226 (2007).

[12] Timothy, C.W., Shaddix, C.R., Schefer, R.W., and Desgroux, P., "The Response of Buoyant Laminar Diffusion Flames to Low-frequency Forcing", *Comb. and Flame*, 151: 676-684 (2007).

[13] Tyagi, M., Jamadar, N., and Chakravarthy, S.R., "Oscillatory Response of an Idealized Two-Dimensional Diffusion Flame: Analytical and Numerical Study", *Comb. and Flame*, 149: 271–285 (2007).

[14] Kuo, K.K., *Principles of Combustion*, John Wiley & Sons, 1986.

[15] Peters, N., *Turbulent Combustion*, Cambridge University Press, 2000.